Liquid phase direct synthesis of H_2O_2: activity and selectivity of Pd-dispersed phase on acidic niobia-silica supports

Antonella Gervasini,[*,§] **Paolo Carniti,**[§] **Frédérique Desmedt,**[#] and **Pierre Miquel**[#,1]

[§] Dipartimento di Chimica, Università degli Studi di Milano, via Camillo Golgi, 19, I-20133 Milano, Italy. E-mail: antonella.gervasini@unimi.it

[#] SOLVAY RD&T GBU Peroxides, Bruxelles, Belgium

[1] Deceased (1982-2016)

ABSTRACT: In this work, acidic niobia-silica (NbS, 4-14 wt.% Nb) materials used as supports of dispersed Pd particles (1.0-2.0 wt.% Pd) have been prepared from different Nb-precursors (niobium ethoxide, NBE, and ammonium niobium oxalate, ANBO) and techniques (co-precipitation and deposition), characterized, and tested in the direct synthesis of H_2O_2 in water and methanol solvents. In particular, on a typical NbS sample, the evolution of morphology (by N_2-adsorption-desorption), crystalline-phase (by XRD), electronic structure (by UV-vis-DRS), and surface acidity with time/temperature of treatment (350-800°C for 4-100 h) has been investigated. Surface acidity was measured by titrations with 2-phenylethylamine adsorption in various liquids: cyclohexane, for the *intrinsic* acidity, and water, methanol, and water-methanol mixtures for the *effective* acidities. Direct H_2O_2 synthesis reaction was performed in semi-batch slurry reactor with continuous feeding of the gaseous mixture (H_2, O_2, and N_2), under pressure ($5 \cdot 10^3$ kPa or 10^4 kPa) at 5°C in methanol or in water. In both solvents, reaction rates only little decreased with time on stream (*ca.* 5% of rate decrease after 4 h of reaction from initial rate of *ca.* 0.5 $g_{H2O2} \cdot (kg_{solution} \cdot min)^{-1}$, according with the slight Pd sintering observed by TEM images. Catalysts prepared by deposition of NBE on silica gave better performances than those prepared from ANBO. In general, selectivity to H_2O_2 in water and in methanol was observed to be similar; the unexpected good selectivity in water was due to the higher *effective* acid strengths of the catalytic surfaces in water than in methanol, as experimentally proven.

INTRODUCTION

Hydrogen peroxide (H_2O_2) is a desirable oxidant because the only by-product from its reduction is water. The largest demand for H_2O_2 is in the pulp and paper industry; in addition, there are applications for H_2O_2 in catalytic oxidations, such as the epoxidation of propene to propylene oxide.[1-3] However, the current production process for H_2O_2, the anthraquinone process, is complex, energy intensive, and only economic for large-scale productions.[4]

The direct synthesis of hydrogen peroxide (H_2O_2 DS) from H_2 and O_2 is an appealing alternative that has the potential to enable small-scale integrated production of H_2O_2.

The catalytic direct synthesis of H_2O_2 is a complex reaction that takes place in a three-phase system and involves two series of parallel and consecutive reactions (Scheme 1). Oxygen in the presence of hydrogen is directly converted either to hydrogen peroxide or to water (simultaneous competitive reactions). The formed H_2O_2 is stable only in an oxidizing atmosphere but can be converted to water in the presence of hydrogen. Therefore, H_2O_2 can be viewed as an intermediate product that can be decomposed or hydrogenated to water (consecutive reactions proceeding in parallel, Scheme 1). In the process, each step proceeds with its own kinetics; various actions have been made to limit, in particular, the two consecutive reactions starting from the hydrogen peroxide formed from the main reaction. Peroxide decomposition can be limited/avoided by introducing acid and/or halides[5-9] with attention for the associated anion of the mineral acid, whose nature can have an influence on reaction activity and selectivity by catalyst poisoning.[10]

The primary catalytic challenge for the H_2O_2 DS reaction is identifying catalysts that can maintain high selectivity for H_2O_2 at industrially relevant H_2O_2 concentrations. The complete reduction of O_2 to H_2O is more thermodynamically favorable than the partial reduction of O_2 to H_2O_2; all the other parallel and consecutive reactions of the process are also thermodynamically favorable reactions.

The optimal DS catalyst must therefore selectively produce H_2O_2 at high rates and preserve H_2O_2 from decomposition. It is currently recognized that the main drawback limiting the catalytic reaction of H_2O_2 synthesis is associated with the poor selectivity to H_2O_2 that can be due to the successive reactions of decomposition, in particular, that of hydrogenation on the formed H_2O_2 giving water (Scheme 1). The stability of H_2O_2 formed strongly depends on the H_2O_2 hydrogenation activity of the used catalysts. The factors that can strongly influence the hydrogenation of H_2O_2 over conventional supported Pd catalysts include: *i*) reaction medium; *ii*) absence/presence of acid or halide ions in the reaction medium; *iii*) H_2/O_2 ratio in the feed; *iv*) catalyst amount, Pd dispersion, and Pd oxidation state;[11] and others

The most extensively studied catalysts are supported palladium or palladium-based multimetallic catalysts. Lunsford and co-workers have extensively worked on palladium-based catalysts, active in H_2O_2 direct synthesis.[12] Catalyst prepared by the colloidal route showed a very high activity in H_2O_2 DS when it is tested in presence of sulfuric acid and halides. Hutchings and co-workers,[13] were the first to show that gold based catalyst (Au/Al_2O_3) was active in the partial reduction of oxygen into hydrogen peroxide They have worked on multimetallic catalysts and, more precisely, on Pd-Au based catalysts (with alumina or carbon black preferably as support).[14] Excellent results are announced without any addition of halides or acids to the medium. However, the catalyst performances were improved by an acid pre-treating the support.[15]

Besides the active phase, support also plays a key role in determining the catalytic performances for H_2O_2 production. The role of support in conversion and selectivity of H_2O_2 DS reaction has been long studied.[16] Numerous support materials of various nature with high surface area (carbons, oxides, zeolites, etc.) have been checked in the H_2O_2 DS. It is known that acidic supports enhance the electron deficiency on the metal particles so favoring the reactant adsorption.[17, 18]

The effect of niobia-silica (NbS) materials on stability of the dispersed Pd active phase has not been already reported, as far as the authors know. Niobia-silica is an interesting mixed oxide that has acidic properties thanks to the presence of tetrahedral or octahedral Nb-species forced in/on the oxide

structure of silica. Excess of negative or positive charge can then be generated in connection to the Si-O-Nb linkages, imparting a more or less strong acid feature to the NbS surfaces.[19, 20] NbS samples have been synthesized in large interval of Nb-concentration by sol-gel synthesis, in particular.[21] The samples possess morphological and chemical properties useful in heterogeneous catalysis and they have been exploited both as support and active phases in various reactions requiring acid sites or redox properties.[22-26] One of the typical feature of Nb-containing oxides is the *water-tolerance* of the acid sites, therefore they have been used in reactions where water is concerned as solvent, reagent, or product.[27, 28]

In this work, a series of NbS samples have been prepared/synthesized and used as supports for Pd dispersed phase to obtain catalysts[29] that have been employed in the H_2O_2 DS reaction. Supports and catalysts have been characterized for some properties that could be in relation with activity: *intrinsic* and *effective* acidity measured in water, methanol, and water-methanol mixtures, texture, and structural properties. In particular, on a selected NbS sample, a series of thermally aged samples have been prepared and thoroughly studied in order to understand the potentiality of this material as support component in a catalyst that has to work in a very severe environment due to the high exothermicity of the H_2O_2 DS reaction. The results here presented should be useful to understand several unknown properties of NbS materials that could be usefully exploited in other reactions.

EXPERIMENTAL SECTION

Support and Pd-Catalyst Preparation. *Chemicals and Materials.* The chemicals used for the support and catalyst preparation: niobium (V) ethoxide (NBE), nitric acid, tetraethyl orthosilicate (TEOS), hexadecyltrimethylammonium bromide (CTAB), tetrapropylammonium bromide (TPAOH, 95%), and palladium(II) chloride, were all commercially available and supplied from Sigma-Aldrich (> 98% purity). Ammonium niobium oxalate complex (ANBO) has been kindly furnished from Companhia Brasileira de Metalurgia e Mineraça, CBMM, Brasil. A commercial silica gel supplied from Aldrich has been also used as support.

NbS Support Preparation. Niobia-silica supports (NbS) have been prepared by *i*) deposition of a molecular precursor of Nb on pre-formed silica powder (sample code D-Nb$_x$S, with x the amount of Nb in percent mass) and *ii*) co-precipitation from molecular Nb- and Si-precursors (sample code P-Nb$_x$S, with x the amount of Nb in percent mass). The NbS samples have been prepared/synthesized with Nb-concentration ranging from 4 to 14 Nb wt.% (Table 1).

The detailed method used for the preparation of niobia-silica with niobium deposition on pre-formed silica described in S.I. paragraph. Summing up, given amount of silica was suspended in dried n-hexane under the nitrogen flow and weighted amount of niobium (V) ethoxide was added. After 3 h under stirring, n-hexane was evaporated at 80°C in a rotary evaporator and the obtained solid was put in a diluted solution of nitric acid (0.5M) for ca. 16 h. After water evaporation, the recovered solid was washed and dried at 100°C for 24 hours.

Synthesized NbS samples from molecular precursors (ANBO or NBE and TEOS) were obtained from co-precipitation methods as described in S.I. paragraph. Aqueous solution of weighted amounts of ANBO or ethanolic solution of weighted pure NBE was dropped into hydrolyzed TEOS (0.05 M, HCl/TEOS=4) in the presence of CTAB surfactant. Then, TPAOH (80 wt.%) was added until complete solid precipitation. After 24 h of ageing, the solid was dried under vacuum at 40°C for 2 h, then at 120°C at atmospheric pressure and calcined at 550°C for 8h.

Tests of ageing of the silica, S, and D-Nb$_{6.4}$S samples (Table 1) at several temperatures (from 350°C to 800°C) for different times (from 4 to 100 h) have been carried out to comparatively study the morphological and structural stability of the thermal aged samples. Around 1 g of sample was put in several ceramic crucibles and inserted in an oven (Nabertherm, Germany, with temperature/time controller B-180) held at constant temperature, under air atmosphere. At given time, the crucibles were taken off and cooled down at room temperature.

The aged samples were called as S/T/t and D-Nb$_x$S/T/t, where "T" is the temperature and "t" the time of sample treatment.

Catalyst Preparation. The incipient wetness method was used for the Pd-deposition on the prepared NbS and S supports, starting from palladium (II) chloride precursor. Details on the preparation can be found in S.I. paragraph. The Pt concentration on all the NbS supports was in the interval 1-2 wt.% Pd.

The catalyst samples have been labelled with the following codes: $Pd_y/D(P)-Nb_xS$, where x is the amount of Nb, in percent mass, and y the amount of Pd, in percent mass, in the sample (Table 1).

Support and Pd-Catalysts Characterization. Inductively coupled plasma optical emission spectrometry analysis (Agilent 720 ES ICP-OES spectrometer) for determining the Nb (emission line at 210.942 nm) and Pd (emission line at 342.122 nm) amounts (ca. 50 mg) in the supports and catalysts were performed as reported in S.I. paragraph.

BET surface area and porosity (pore volume, pore size, and pore distribution) have been determined by collecting N_2 adsorption-desorption isotherms at -196 °C using a Sorptomatic 1900 instrument (Carlo Erba). Pore volume distribution was calculated from the desorption branch of the isotherms using the Barrett-Joyner-Halenda (BJH) model equation. Prior to the analysis, the fresh, aged, and used supports and catalysts in amount from 0.2 to 0.3 g were outgassed under vacuum at 150°C for 16 h.

Scanning electron micrographs (SEM) have been obtained by a LEO 1530 coupled with energy dispersive X-ray spectroscopy (EDS) analyzer working at 20 keV. The samples were analyzed under a moderate vacuum after gold coating.

Transmission electron microscopy (TEM) analysis was performed with a Zeiss LIBRA® 200FE, equipped with 200 kV FEG, in column second-generation omega filter for energy selective spectroscopy (EELS) and imaging (ESI), HAADF, STEM facility, EDS probe for chemical analysis, integrated tomographic HW and SW system. Samples were prepared by dropping a suspension of silica-based samples in isopropanol on a holey carbon copper grid (300 mesh) and evaporating the

solvent. Histograms of the particle size distribution were obtained by counting onto the micrographs at least 300 particles; the mean particle diameter (d_m) was calculated by using the formula:

$d_m = \Sigma\, d_i\, n_i / \Sigma\, n_i$

where n_i was the number of particles of diameter d_i.

X-ray diffraction (XRD) patterns of the powder samples have been recorded with a Philips PW3020 diffractometer using a CuKα radiation ($\lambda = 1.541874$ Å) and fixed power source (40 kV and 40 mA) with step size of 0.020 θ. The samples were scanned at a rate of 1degree·min^{-1} (2θ) over a range of 5-60 °θ, which comprises the characteristics diffraction peaks of various crystalline niobium oxide phases.

UV-vis diffuse reflectance spectroscopy (UV-vis-DRS) measurements were performed on the samples (non-diluted powders) put into a cell with optical quartz walls in a Perkin-Elmer Lambda 35 instrument equipped with an integrating sphere and Spectralon©, as reference material. The spectra were measured in absorbance mode and then reconverted in Schuster Kubelka-Munk function, $F(R\infty)$. The edge energy values (E_g) were determined by finding the intercept of the straight line in the low-energy rise of a plot $[F(R\infty)\cdot h\nu]^2$ against $h\nu$ (incident photon energy).

Apparatus and procedure for the determination of sample acidity by the pulse technique. Experiments were performed in a liquid chromatograph (HPLC) line especially modified for performing acid-base titrations in liquid-solid phase.[30, 31]

For each experiment, a weighed amount (*ca*. 0.030 g) of fresh sample was treated at 150°C under flowing air for 4 h, then, it was evacuated and filled with the liquid (cyclohexane for the *intrinsic* acidity or methanol or water or methanol-water mixture for the *effective* acidity) under vacuum. In each adsorption test, pulses (50 μl) of PEA solution of known concentration were sent at fixed time intervals (15 min) onto the sample maintained at a constant liquid flow rate (5 ml/min). The non-adsorbed amounts of PEA after each pulse were detected up to sample saturation. A typical example of obtained chromatogram for PEA adsorption onto a catalyst sample is depicted n Figure S1.

Computations to determine the amount of acid sites titrated by amine adsorption have been reported in S.I. paragraph.

On each sample, adsorption of PEA was repeated two times (I run and II run), the two runs were interspaced by the pure liquid elution (30 min). The strong acidity of the sample was obtained by subtracting the acid sites titrated in the II run (weak acid sites) from those of the I run adsorption (total acid sites).

Catalytic tests of DS H_2O_2 synthesis. Chemicals and solvents used (hydrobromic acid, methanol, and water) were all supplied by Sigma-Aldrich and VWR.

The installation used for the H_2O_2 DS tests in liquid-phase worked at 5°C in semi-batch configuration (Figure 1). During a test, the hastelloy-22 reactor was flushed continuously with the gaseous mixture which was analyzed by gas chromatograph (Shimadzu, GC14B, equipped with thermal conductivity detector and Molecular Sieves column) put on line at the reactor outlet. The products (hydrogen peroxide and water) accumulated in the reactor during the test and were analyzed regularly through liquid samples.

In a standard test procedure, 150 g of methanol (99%), or 100 g of water, *ca.* 1.50 g of catalyst sample, and some drops of methanolic solution of HBr (ca. 30 ppm) were introduced in the reactor maintained at $5 \cdot 10^3$ kPa (for tests in methanol) or 10^4 kPa (for tests in water) with N_2 flow. Oxygen and hydrogen were introduced in the reactor (O_2 flow, 1490 Nml·min^{-1} and H_2 flow, 98 Nml·min^{-1}), in order to reach a maximum hydrogen concentration of 3.6 vol.%.

Determination of water was done by Karl Fisher titration with MetrOhm equipment. Hydrogen peroxide determination was done by oxido-reduction titration with cerium sulfate in slightly acid conditions. Selectivity to H_2O_2 was calculated from the amount of H_2O_2 measured at given times of sampling ($g_{H2O2}·kg_{solution}^{-1}$) in comparison with the amount of H_2 converted.

All other details on the installation, operative procedure, and analytical analyses can be found in S.I. paragraph.

RESULTS AND DISCUSSION

With the intent to prepare support materials for dispersing Pd-phase that has to be active and selective during the H_2O_2-DS reaction, a series of niobia-silica (NbS) samples with different amounts of Nb (from 4 to 14 wt.%) have been prepared.

Several P-NbS samples have been prepared starting from ANBO or NBE as Nb-precursors and TEOS, as Si-font and several D-NbS samples by deposition of NBE on a finite silica support material (Table 1). The co-precipitation method was already used with success to prepare several silica-niobia catalysts for use in reactions of dehydration of sugars.[21] It was expected that different morphological and acidic properties characterize the samples of the two series. In the case of the sample series prepared by deposition, almost the totality of Nb loaded on silica is present at the surface, while only part of the Nb is present on the surface (and part in the bulk), in the case of the sample series prepared by co-precipitation. This had been observed on a series of silica-niobia samples prepared by co-precipitation, by comparing the Nb/Si ratio, determined by XPS, with the bulk Nb/Si ratio.[21] In any case, high surface area and porosity and surface acidity are desired properties of the NbS support samples, in order to stably anchor the active Pd-phase deposited on the NbS supports.

On the NbS samples, dispersed Pd phase at low concentration (from 1 to 2 Pd wt.%.) has been deposited by conventional wetness impregnation method starting from palladium (II) chloride salt. The obtained catalyst samples ($Pd_y/D(P)$-Nb_xS) are listed in Table 1 with their composition.

Morphological properties of P-NbS and D-NbS samples and of silica (S) are collected in Table 2, which reports the results obtained from N_2 adsorption/desorption isotherms. The morphology of the D-NbS samples was governed by the morphology and texture of silica, while that of P-NbS samples was affected by the nature of the chemical precursor used.

The surface area value of silica was in the range of the typical mesoporous materials (304 $m^2 \cdot g^{-1}$) with well-developed porosity (1.16 $mL \cdot g^{-1}$ and 15.3 nm of pore size) (Figure S2). Deposition of

Nb on S did not cause remarkable decrease of surface area of the resultant samples; D-Nb$_{6.4}$S and D-Nb$_{7.3}$S have slightly higher surface area than bare S, while D-Nb$_9$S, with the highest amount of Nb among the samples prepared by deposition, has slightly lower surface area than bare S (Table 2). Porosity of S was maintained for the three D-NbS samples, D-Nb$_{6.4}$S and D-Nb$_{7.3}$S and D-Nb$_9$S with only a slightly decrease of pore volume and average pore size (Table 2). From the obtained morphological results, it can be inferred a good dispersion of Nb on the silica surface for all the three samples, D-Nb$_{6.4}$S and D-Nb$_{7.3}$S and D-Nb$_9$S, obtained by the deposition method. The NbS samples prepared by co-precipitation have decreasing surface area values with increasing Nb-concentration. High surface area values of the silica-niobia materials are associated with the presence of Si–O–Nb linkages. The samples prepared by NBE precursor at 6.2 and 14.2 Nb wt.% maintained both high surface area (436 and 294 m$^2 \cdot$g^{-1}, respectively). Conversely by using ANBO as Nb-precursor, the values of surface area deeply decreased with increasing Nb-concentration (436 and 71 m$^2 \cdot$g^{-1} for 4 Nb wt.% and 6.5 Nb wt.%, respectively) (Table 2). This behavior was already noticed on several silica-niobia samples prepared from ANBO as Nb-precursor.[21] Silica could accommodate niobium up to a given concentration, when the threshold is overcome, niobium agglomeration occurs with dramatic change of the textural properties of the samples. Porosity of the P-NbS samples prepared from NBE was much higher than that of samples prepared from ANBO as Nb-precursor. This observation indicates that by preparing NbS samples from ANBO in water, it is not possible to create Si–O–Nb linkages imparting good morphological properties to the samples. SEM images of typical NbS samples prepared by deposition and co-precipitation are shown Figure S3.

Characterization of D-Nb$_{6.4}$S sample. The surface properties of NbS supports are of great importance in order to stabilize the Pd dispersed phase during its work in the severe conditions under which the H$_2$O$_2$ DS reactor works. H$_2$O$_2$ DS reaction is highly exothermic ($\Delta H_{298\ K}$ = 135.9 kJ$\cdot$mol^{-1}) and the catalyst surface undergoes to serious hot spots in the zone in which Pd-clusters are present.

This could lead to Pd aggregation with loss of Pd dispersion and modification of activity/selectivity of reaction with time, if Pd clusters are not tenaciously tied to the support surface.

With this in mind, we have performed a thorough characterization analysis on D-Nb$_{6.4}$S, chosen as representative sample among the prepared D-NbS samples. The morphological and structural properties of D-Nb$_{6.4}$S have been studied as a function of thermal treatment to investigate on the thermal stability of the sample. Moreover, the surface chemical properties (*intrinsic* and *effective* acidity) of D-Nb$_{6.4}$S were determined under different liquid environments (water, methanol, and water-methanol mixture) to mimic the real conditions of reaction. Concerning the characterization of silica-niobia samples prepared by co-precipitation from aqueous solution, the results of several features of such samples prepared at various Nb-concentrations can be found in Ref. **21**.

For D-Nb$_{6.4}$S, the N$_2$ adsorption and desorption isotherms and relevant pore size distribution obtained from the desorption branch of the N$_2$ isotherms are depicted in Figure 2. D-Nb$_{6.4}$S is a typical mesoporous sample (type IV isotherm) with a large hysteresis (from 0.7 to 0.9 P/P°) typical of well-defined cylindrical-like pore channels or agglomerates of approximately uniform spheres (H1, following IUPAC classification). D-Nb$_{6.4}$S possessed an almost unique pore size distribution centered at ca. 10-12 nm of size. The morphological characteristics of D-Nb$_{6.4}$S are governed by the morphology of silica over which NBE has been deposited.

To comparatively study the morphological and structural stability of S and D-Nb$_{6.4}$S, thermal aged samples have been prepared by treating portions of the two fresh samples at several temperatures (from 350°C to 800°C) for different times (from 4 to 100 h). The aged-samples have been successively analyzed for determining surface area and porosity (N$_2$ adsorption/desorption isotherms, structure (XRD), spectroscopic properties (UV-vis), and *intrinsic* surface acidity (amount of acid sites). Figures 3 and 4 show the trends of surface area evolution of S (Figure 3) and D-Nb$_{6.4}$S (Figure 4) samples treated at temperatures of 350°, 500°C and 800°C as a function of time (up to 100 h). The surface area values of S treated both at 350°and 500°C are unaffected in comparison with that of fresh silica sample (304 m^2·g^{-1} after treatment at 150°C), same independently of temperature and time of

the thermal treatment, while a marked decrease of surface was observed for treatment at 800°C. A regular exponential decrease of surface area with time of treatment was noticed; after 30 h of thermal treatment (S/800/30), the value of surface area was as low as 34 $m^2 \cdot g^{-1}$. A completely different situation emerged when the aged D-$Nb_{6.4}$S samples (from 350°C to 800°C for time up to 100 h) have been studied (Figure 4). The D-$Nb_{6.4}$S samples treated at 350°C have values of surface area very similar or even higher than the fresh sample (311 $m^2 \cdot g^{-1}$ after treatment at 150°C). For treatment at 500°C, only slight decrease of the values could be observed ($Nb_{6.4}$S/500/60 has 300 $m^2 \cdot g^{-1}$ of surface area). Quite surprisingly, the decreasing trend of surface area evolution with time for heat treatment at 800°C was very small. D-$Nb_{6.4}$S/800/30 maintained more than 85% of surface area of the fresh sample (268 $m^2 \cdot g^{-1}$ of surface area); this behavior is even more unexpected if compared with the surface area of S/800/30 (34 $m^2 \cdot g^{-1}$). In parallel, the pore volume of D-$Nb_{6.4}$S was maintained also for the aged samples treated at 800°C (pore volume of D-$Nb_{6.4}$S/800/30 was 0.956 $mL \cdot g^{-1}$). The extraordinary properties of morphological stability of D-$Nb_{6.4}$S with temperature are likely due to the Nb-O-Si linkages formed at the surface that prevent the sintering of the bulk material.

A structural investigation (by XRD) was performed on the aged S and D-$Nb_{6.4}$S samples, to study the consequences induced by temperature on phase transformation of the samples. Both fresh S and D-$Nb_{6.4}$S samples were amorphous. Silica maintained amorphous properties for thermal treatment at 500°C and also for treatment at 800°C for 8 h. For longer time treatment at 800°C, silica was completely converted to α-cristobalite (JCPDS 01-082-1235), a high-temperature polymorph of silica (Figures S4a and S4b). Also fresh D-$Nb_{6.4}$S was amorphous; for treatment at 800°C for 8 h, little amount of crystalline phase appeared. This phase grew for longer time treatment at 800°C. On D-$Nb_{6.4}$S/800/30, it was visible a crystalline phase that could be associated with Nb_2O_5 (JCPDS 00-037-1468) (Figures S4c and S4d); the presence of large diffraction peaks of Nb_2O_5 of low crystallinity covered the sharp diffraction peak of α-cristobalite phase silica, which formed at such high temperature. Summarizing, thermal treatment of D-$Nb_{6.4}$S at high temperature for long time caused a coexistence of amorphous and crystalline phases.

To complete the characterization of the fresh and aged D-Nb$_{6.4}$S samples, electronic spectroscopy (UV-vis-DRS) was used, aimed to detect the modification of Nb electronic properties and Nb-coordination with oxygen atoms around it. Figure 5 shows all the UV-vis-DR spectra of D-Nb$_{6.4}$S thermally treated at 350° (Figure 6 A), 500° (Figure 5 B), and 800°C (Figure 5 C) for different time, presented as absorbance against wavelength. For wavelength higher than 400 nm, any electronic band was not visible. At lower wavelength region observed, the only bands were due to ligand-to-metal charge transfer transitions (LMCT from O^{2-} to Nb^{5+}) without possibility to distinguish the Nb-coordination, tetrahedral (230 nm) or five- and six-coordinated Nb species at ca. 250 nm.[32] The thermally treated D-Nb$_{6.4}$S samples are not markedly different among them, neither in terms of intensity nor in terms of appearance of new transitions (e.g., a band centered at 320 nm, typical of nano-aggregated of Nb$_2$O$_5$). At each temperature, a representative sample was chosen for showing the Tauc-plot (350°C, Figure 5A'; 500°C, Figure 5B'; 800°C, Figure 5C'), to calculate the absorption edge energy and band gap energy, E$_g$. The calculated E$_g$ values are all in a little interval of values (3.4-3.15 eV), with very slight decreasing trend with time of pretreatment for each temperature. This indicated that the formed Nb$_2$O$_5$ phase did not undergo to a rapid sintering with temperature; the high temperatures and times of treatment of D-Nb$_{6.4}$S caused a limited polymerization of the NbO$_x$ units over the silica surface.

One of the desired properties of the NbS samples in view of their use as supports of Pd-dispersed phase in the DS H$_2$O$_2$ reaction was surface acidity. *Intrinsic* acidity of D-Nb$_{6.4}$S was measured in cyclohexane with PEA as base probe molecule by a pulse titration flow method that exploits a liquid chromatography to realize the titration.[30, 31] The results obtained from the acid-base titration of fresh and aged D-Nb$_{6.4}$S are presented in Figure 6 and in Table 3. Fresh D-Nb$_{6.4}$S sample is highly acidic with sites of high acid strength, about 83% of the titrated acid sites remained still covered by PEA as observed by comparing I° and II° run adsorptions, interspaced by flowing pure cyclohexane at the same temperature. Acidity was maintained without appreciable decrease on aged D-Nb$_{6.4}$S sample treated at 350°C for 100 h (Table 3). The amount of acid sites regularly decreased for higher

temperatures of treatment (500° and 800°C), in parallel with a slight decrease of the strong acidity. Anyway, it is worth noticing that D-Nb$_{6.4}$/800/30, maintaining an important surface area (268 m^2·g^{-1}), maintains also good acidity (350 μequiv·g^{-1} of total acid sites, 76% of which are strong sites).

On fresh D-Nb$_{6.4}$S, *effective* acidity was also measured to investigate the ability to maintain acidity in real conditions of use during H$_2$O$_2$ DS reaction. Acid-base titrations with PEA were carried out in water, in methanol, and in various water-methanol mixtures. The results of the titrations are presented in Figure 7. The acidity of D-Nb$_{6.4}$S was in part maintained in water (244 mequiv·g^{-1}, about 50% of the acid sites titrated in in cyclohexane). This indicated the *water-tolerance* of part of the acid sites of D-Nb$_{6.4}$S, likely the acid sites associated with Nb centers. The observed loss of ca. 50% of acidity, it is likely to be associated with acid sites of silica that are so weak that they could not be titrated in water. If one compares the slopes of the curves of acid-base titrations of D-Nb$_{6.4}$S obtained in cyclohexane and in water, it emerges the higher slope of the curves in cyclohexane (Figure 6) than in water (Figure 7). This suggests that the average acid strength of D-Nb$_{6.4}$S is higher in cyclohexane than in water. However, the good *effective* acidity of D-Nb$_{6.4}$S sample can be helpful for anchoring the Pd-phase and minimizing its sintering during reaction.

The addition of given amount of methanol to water had important consequences on the surface acidity of D-Nb$_{6.4}$S (Figure 7). The *effective* acidity of D-Nb$_{6.4}$S in water-methanol solutions was very lower than in water. A solution containing 15% wt.% of methanol in water caused the loss of ca. one third of the acid sites of D-Nb$_{6.4}$S titrated in water (Figure 8). Further addition of methanol in water (30%, 50% and 70% wt.%) caused a little regular decreasing trend of acidity of D-Nb$_{6.4}$S. The *effective* acidity of D-Nb$_{6.4}$S in almost methanol (97% wt.% of methanol in water) was very little. The coordination of methanol to Nb(V) sites, likely through adsorbed methoxy species, was so strong that PEA probe could not displace methanol and substitute it in coordination to Nb(V). Figure 8 enlightens the deep decreasing trend of the acid sites of D-Nb$_{6.4}$S titrated with PEA in water-methanol solutions as a function of molar fraction of methanol. In Figure 8, both total titrated acid sites and

strong acid sites against methanol molar fraction are shown, the two types of acid sites are almost coincident between them, confirming that only the strong sites can be titrated in such environment.

In our knowledge, it is the first time that such evidence is reported in the literature, that Nb-acid sites of mixed niobia-silica samples are not *methanol-tolerant*, which means that effective acidity of Nb-sites in methanol is (almost) completely lost. This behavior has important consequences in the catalytic performances of materials containing niobium, as enlightened by Ziolek and coworkers.[33-34] The presence of niobium in the studied catalysts[33-34] deeply modified the products profile and markedly influenced the selectivity in the methanol oxidation reaction. Strongly adsorbed methoxy species played a key role in the selectivity and product distribution, giving rise to higher amounts of formaldehyde.

Pd/NbS Catalyst and Activity in H_2O_2 DS reaction. Pd/NbS catalysts have been prepared starting from different NbS samples on which amounts from 1 to 2 wt.% of Pd have been added from $PdCl_2$ precursor. In general, the morphological features of Pd/NbS did not differ from those of the relevant NbS support. For example, $Nb_{7.3}S$ and $Pd_{1.6}Nb_{7.3}S$ have 310 and 296 $m^2 \cdot g^{-1}$ of surface area, respectively, and both have around 1.00 $mL \cdot g^{-1}$ of pore volume; and Nb_9S and $Pd_{1.4}Nb_9S$ have 279 and 281 $m^2 \cdot g^{-1}$ of surface area, respectively, and both have around 1.00 $mL \cdot g^{-1}$ of pore volume. These observations suggest that fine dispersion of Pd, without modification of support morphology, has been achieved. Concerning acidity, in general Pd/NbS catalysts are more acidic surfaces than the related NbS samples, this is because the deposition procedure of Pd on NbS support employed an acid solution of Pd(II) chloride into which NbS support was put. Acid solution with mineral acid, likely provoked hydrolysis of surface X-O-Y (X, Y = Si, Nb) with formation of X-OH and Y-OH acidic groups. For example, the *intrinsic* acidity (measured in cyclohexane) of D-$Nb_{7.3}S$ and $Pd_{1.6}/D(P)$-$Nb_{7.3}S$ was equal to 620 and 725 $\mu equiv \cdot g^{-1}$ of acid sites, respectively; and the *intrinsic* acidity of Nb_9S and $Pd_{1.4}Nb_9S$ was equal to 480 and 520 $\mu equiv \cdot g^{-1}$ of acid sites, respectively.

All the H_2O_2 DS reactions were performed in a semi-batch reactor working at 5°C with 1.50 g of catalysts under very higher flow rate of oxygen than hydrogen in two different solvents, methanol

and water; reaction was observed for 250 min during which reagents and products were analyzed. The tests were aimed at controlling the H_2 conversion and H_2O_2 selectivity during time and at comparing the catalyst activity in connection with the different NbS support composition and/or the different NbS support preparations.

A typical example of the results obtained in terms of profiles of reagents/products against time on stream is shown in Figure 9. During the time of observation and under the experimental conditions used (in particular, H_2, 3.6 vol.% in the reactor) the following general observations were made. Hydrogen conversion was always observed between 40-60% with only a very slightly decreasing trend with time. Peroxide selectivity started always very high (close to 100%) and then, more or less, declined with time. This signifies that the two parallel reactions (giving rise to H_2O_2, k_1, and H_2O, k_{20} in Scheme 1) are not in competition; the rate of reaction from H_2 and O_2 to H_2O has a much lower rate than that forming H_2O_2. Therefore, selectivity to H_2O_2 mainly depends on the consecutive reactions from the H_2O_2 formed (Scheme 1). It was generally observed that peroxide and water concentrations regularly increased at constant rate (in general, 0.4-0.5 $g_{H2O2} \cdot (kg_{solution} \cdot min)^{-1}$ and *ca*. 0.1 $g_{H2O} \cdot (kg_{solution} \cdot min)^{-1}$) with time. For time of reaction higher than 6 h, the concentration profiles of H_2O_2 and H_2O incurved, indicating more or less deactivation of catalyst activity. The results observed were similar in water and in methanol but the trend of H_2O_2 selectivity with time on stream, in particular, slightly changed on different catalyst samples.

H_2O_2 DS Catalytic Tests in Methanol and in Water. Chosen examples of H_2O_2 DS tests in methanol are shown in Figures 10 and 11. They present the performances of four different Pd/NbS catalysts. In Figure 10, the H_2 conversion and H_2O_2 selectivity of two catalysts prepared by co-precipitation from ANBO and TEOS as Nb- and Si-precursors at different Nb content and similar Pd-concentration are compared: $Pd_{1.0}/P$-Nb_4S and $Pd_{1.2}/P$-$Nb_{6.5}S$. The H_2 conversion lines with time of $Pd_{1.0}/P$-Nb_4S and $Pd_{1.2}/P$-$Nb_{6.5}S$ run almost parallel, around 30% and 40%, respectively, with very slightly negative slopes. The line of the sample containing higher amount of Pd lies above, as expected, that is, $Pd_{1.2}/P$-$Nb_{6.5}S$ has higher catalytic activity, thanks to the higher Pd concentration.

The H_2O_2 selectivity lines are more sloped than the H_2 conversion lines and also in this case, they run almost parallel, the line of $Pd_{1.2}/P-Nb_{6.5}S$ lying above that of $Pd_{1.0}/P-Nb_4S$. Clearly, the two catalysts have very similar performances in the H_2O_2 DS reaction, and they both loose selectivity to H_2O_2 with time. In Figure 11, the catalytic performances of $Pd_{1.6}/D-Nb_{7.3}S$ and $Pd_{1.4}/D-Nb_9S$ catalysts have been compared, both have been prepared by deposition of NBE, as Nb-precursor, on silica. Higher H_2 conversions are observed than those shown in Figure 10, thanks to the higher Pd-concentrations in the catalysts. In this case, the H_2 conversion line of $Pd_{1.4}/D-Nb_9S$ lies over that of $Pd_{1.6}/D-Nb_{7.3}S$; this suggested that Pd-dispersion, and not Pd-concentration, governed the catalytic activity. Likely, Pd-dispersion does not run in parallel with Pd-concentration, starting from a given threshold of amount of Pd added, as well known.[35-36] In this case, H_2O_2 selectivity values started very high and then only slightly declined with time. Comparing H_2O_2 selectivity lines as a function of time, higher selectivity is associated with the more active catalyst ($Pd_{1.4}/D-Nb_9S$).

The H_2O_2 DS reaction was also performed in aqueous solutions. In this case, reaction took place under higher pressure than in methanol (10^4 kPa in water vs. $5 \ 10^3$ kPa in methanol) in order to increase the H_2 and O_2 solubility that are known to be very lower in water than in alcoholic solvents.[16] It is generally accepted that the rate of H_2O_2 production in alcoholic medium is much higher than that in aqueous medium; thanks to the increased mass transfer of the reactant gases in solution (solubility of H_2 in alcohol is 4-5 times higher in methanol than in water at room temperature). In addition, selectivity to H_2O_2 in water is considered much lower than in methanol, because the rate of H_2O_2 conversion in the presence of hydrogen in aqueous medium is much higher than that in methanol, even though hydrogen solubility is higher in methanol than in water. According with Melada et al.,[37] in methanol the formation of formate species can block the most active Pd-sites responsible of the HO-OH bond breaking (hydrogenation activity).

Surprisingly, our observations indicated that selectivity to H_2O_2 in aqueous medium was similar to that observed on the most selective catalysts in methanol. As an example, Figure 12 shows the results of H_2O_2 DS reaction in water on two catalysts ($Pd_{1.4}/P-Nb_{14.2}S$ and $Pd_{1.9}/P-Nb_{6.2}S$), both

prepared by co-precipitation from NBE and TEOS as Nb- and Si-precursors, respectively. In aqueous solution on the two catalysts, H_2 conversion run around 31-38% with very high stability. H_2O_2 selectivity, after a first decreasing during the first 60 min of reaction, was also very stable, around 88-90%. The interesting positive results for the H_2O_2 DS reaction in aqueous solution are enlightened by comparing the results obtained in methanol and in water after 4 h of reaction over $Pd_{1.9}/P-Nb_{6.2}S$ and $Pd_{1.2}/P-Nb_{6.5}S$ catalysts (Figure 13). The two catalysts were both prepared from co-precipitation and they contain similar Nb-concentration in the NbS support. They were prepared from two different Nb-precursors: $Pd_{1.2}/P-Nb_{6.5}S$ was prepared from ANBO and $Pd_{1.9}/P-Nb_{6.2}S$ from NBE. $Pd_{1.2}/P-Nb_{6.5}S$, as already observed in Figure 10, worked in methanol with poor activity and selectivity to H_2O_2. $Pd_{1.9}/P-Nb_{6.2}S$ worked in water with low conversion but with interesting selectivity to H_2O_2 (ca. 85%). This comparison confirmed the superior activity of Pd/NbS catalysts prepared from NBE over those prepared from ANBO, as Nb-precursor. Even if $Pd_{1.2}/P-Nb_{6.5}S$ was tested in methanol, where higher reaction rates than in water are usually observed, its catalytic performances are lower than that of the sample prepared from NBE and tested in water, where low gas solubility prevents obtaining high conversion.

Fresh and used Pd/NbS catalyst characterization.

In general, on the selected Pd/NbS catalysts on which morphological analyses and acidic measurements have been carried out after use in H_2O_2 DS reaction, any remarkable difference with the fresh counterpart was not observed. As example, surface area values of used and fresh $Pd_{1.6}/D-Nb_{7.3}S$ was 310 and 296 $m^2 \cdot g^{-1}$, respectively. In general, the Pd/NbS acidity of the used catalysts was slightly different from that of the fresh samples. For example, *intrinsic* acidity of used $Pd_{1.6}/D-Nb_{7.3}S$ decreased of ca. 20% and *effective* acidity, measured in water, increased of ca. 20%, and *effective* acidity measured in methanol, was confirmed to be almost absent.

The fresh and used NbS and related Pd/NbS catalysts have been studied by micrographic analyses (TEM and STEM) to investigate modification and damages caused to the support and Pd-supported phase by the highly exothermic H_2O_2 DS reaction. We report, as example, the results obtained on D-

$Nb_{7.3}S$ and $Pd_{1.6}/D$-$Nb_{7.3}S$, which has emerged as one of the best catalysts among those tested in the H_2O_2 DS, even if it gave slight decrease of H_2O_2 selectivity during reaction. (see Figure 11).

Figure 14 compares the fresh and used $Pd_{1.6}/D$-$Nb_{7.3}S$ catalysts by significant collected TEM images. General morphology of the particles did not appear modified/damaged after use in the DS reaction; concerning Pd-distribution, some relevant differences emerged. On fresh $Pd_{1.6}/D$-$Nb_{7.3}S$ (Figure 14A), besides some well visible Pd-particles of ca. 5 and 10 nm of size, it is hard to individuate the numerous and smaller Pd-particles which are well distributed over silica surface. Figure 14A' reports the computed Pd-particle size distribution, that indicates the sharp size of Pd-particles at the surface of the fresh catalyst; the most part of the Pd-population was comprised within 5 nm of size. After use, the $Pd_{1.6}/D$-$Nb_{7.3}S$ surface shows more clearly distinguishable Pd-particles of higher dimension well distributed over the silica surface (Figure 14B). The computed Pd particle size distribution is broader in comparison with that of the fresh catalyst. The Pd-population is now centered around 12 nm of size (Figure 14B'). The modest Pd-sintering observed justifies the stable activity and selectivity values obtained on Pd/P-NbS catalysts (in particular catalysts prepared from from NBE precursor).

CONCLUDING REMARKS

Defined Pd/NbS catalysts were prepared by depositing Pd on different niobia-silica materials prepared from different Nb-precursors and by various methods (deposition and co-precipitation) for the use in H_2O_2 DS reaction. NbS supports prepared by deposition from niobium ethoxide on pre-formed silica created robust materials form morphological and structural points of view able to be stable following high temperature treatments.

The *intrinsic* acidity of the NbS samples was well developed and it was found that the acid sites were *water tolerant*, while the samples lost acidity in the presence of methanol. It could then be guessed that the average acid strength of the surfaces was higher in water than in methanol, with consequences on activity/selectivity of the H_2O_2 DS reaction. On Pd/NbS catalysts, selectivity to

H_2O_2 in water was similar to that observed in methanol, in spite of the literature evidences. The high *effective* acidity of the NbS supports in water could enhance the electron deficiency of Pd metal particles, so favoring the reactant adsorption on them. Moreover, on higher acidic catalytic surfaces, the electron transfers, heterolytic H_2 oxidation and O_2 reduction steps occurring while conserving charge, could be favored, as proposed by Wilson and Flaherty.[38] All this acted positively for the selectivity of H_2O_2 reaction in water.

Finally, on the basis of our findings, Pd/Nbs could be considered promising catalysts for the H_2O_2 synthesis reaction realized in water, which is a *friendly* solvent, with the possibility to develop a green synthetic process.

ASSOCIATED CONTENT

Supporting Information

The Supporting Information is available free of charge on the ACS Publications website.

Details on preparationsof D-NbS and P-NbS samples; preparation of Pt/NbS catalysts; ICP analysis; acidity measurements; catalyst testing equipment and method.

Figures of chromatographic peaks obtained in the acid-base titrations of NbS sample with PEA probe during the 1st and 2nd runs experiment; N_2 adsorption/desorption isotherms on silica, S, and pore size distribution and pore volume as a function of pore radius; powder XRD spectra of fresh and aged silica samples; SEM images of chosen P-NbS and D-NbS samples; TEM images of chosen D-NbS sample; STEM and atomic map of chosen D-NbS sample.

AUTHOR INFORMATION

Corresponding Author

* Antonella Gervasini, Tel. +390250314254, E-mail: antonella.gervasini@unimi.it.

ORCID

Antonella Gervasini: 0001-6525-7948

Notes

The author declares no competing financial interest.

AUTHOR CONTRIBUTIONS

A.G. and P.C. designed and performed the experiments of characterization (morphological, structural, spectroscopic analysis as well as the measurements of acidity in liquids) and analysed the data with numerical interpretation. F.D. and P.M. designed and performed the preparation of support materials and catalysts and the catalytic experiments of hydrogen peroxide synthesis. A.G. performed the coordination of the work and of the preparation of the manuscript with input from all the other authors.

REFERENCES

(1)   Walsh, P.B. *Tappi Journal*, **1991**, *74*, 81–83.

(2)   Strukul, G., Ed.; *Catalytic Oxidations with Hydrogen Peroxide as Oxidant*. Kluwer Academic; Dordrecht, The Netherlands: 1992.

(3)   Nijhuis, T.A.; Makkee, M.; Moulijn, J.A.; Weckhuysen, B.M. *Ind. Eng. Chem. Res*. **2006**, *45*, 3447–3459.

(4)   Centi G, Perathoner S, Abate S. In *Modern Heterogeneous Oxidation Catalysis,* Mizuno N., Ed.; Wiley-VCH; Weinheim, Germany: 2009; pp. 253–287.

(5)   Liu, Q.; Lunsford, J.H. *Appl. Catal., A* **2006**, *314*, 94-100.

(6)   Choudhary, V.R.; Samanta, C.; Jana, P. *Appl. Catal., A* **2007**, *317*, 134-243.

(7)   Choudhary, V.R.; Samanta, C.; Jana, P. *Appl. Catal., A* **2007**, *332*, 70-78.

(8)   Choudhary, V.R.; Jana, P. *J. Catal.* **2007**, *246*, 434-439.

(9)   Han, Y.; Lunsford, J.H. *J. Catal.* **2005**, *230*, 313-316.

(10) Choudhary, V.R.; Samanta, *J. Catal.* **2006**, *8,* 28-38.

(11) Olivera, P.P.; Patrito, E.M.; Sellers, H. *Surf. Sci.* **1994**, *313*, 25-40.

(12) Liu, Q.; Bauer, J.C.; Schaak, R.E.; Lundsford, J.H. *Angew. Chem., Int. Ed*. **2008**, *47*, 6221-6224.

(13) Edwards, J.K.; Hutchings, G.J. *Angew. Chem., Int. Ed.* **2008***, 47*, 9192-9198.

(14) Edwards, J.K.; Freakley, S.J.; Lewis, R.J.; Pritchard, J.C.; Hutchings, G.J. *Catal. Today* **2015**, *248*, 3-9

(15) Edwards, J.K.; Parker, S.F.; Pritchard, J.C.; Piccinini, M.; Freakley, S.J.; He, Q.; Carey, A.F.; Kiely, C.J.; Hutchings, G.J. *Catal. Sci. Technol.* **2013**, *3*, 812-818.

(16) Samanta, C. *Appl. Catal., A* **2008**, *350,* 133-149.

(17) Ishihara, T.; Harada, K.; Eguchi, K.; Arai, H. *J. Catal.* **1992**, *136,* 161-169.

(18) Stakheev, A.Y.; Kustov, L.M.; *Appl. Catal., A* **1999**, *188*, 3-35.

(19) Gervasini, A.; Fenyvesi, J.; Auroux, A. *Langmuir* **1996**, *12*, 5356-5364.

(20) Tanabe, K.; Misono, M.; Ono, Y.; Hattori, H. In *Studies in Surface Science and Catalysis,* Delmon, B.; Yates, J.T. Ed.s; Kodansha, Tokyo, 1989; Vol. 51.

(21) Carniti, P.; Gervasini, A.; Marzo, M. *J. Phys. Chem.* C **2008**, *112*, 14064-14074.

(22) Carniti, P.; Gervasini, A.; Biella, S.; Auroux, A. *Catal. Today* **2006**, *118*, 373-378.

(23) Aronne, A.; Marenna, E. Califano, V.; Fanelli, E.; Pernice, P.; Trifuoggi, M.; Vergara, A. *J. Sol-Gel Sci. Technol.* **2007**, *43*, 193-204.

(24) Aronne, A.; Turco, M.; Bagnasco, G.; Ramis, G.; Santacesaria, E.; Di Serio, M.; Marenna, E.; Bevilacqua, M.; Cammarano, C.; Fanelli, E. *Appl. Catal., A* **2008**, *347*, 179-185.

(25) Wachs, I.E.; Jehng, J.M.; Deo, G.; Hu, H.; Arora, N. *Catal Today* **1996**, *28*, 199-205.

(26) Dragone, L.; Moggi, P.; Predieri, G.; Zanoni, R. *Appl. Surf. Sci.* **2002**, *187*, 82-88.

(27) Okuhara, T. *Chem. Rev.* **2002**, *102*, 3641-3666.

(28) Ziolek, M. *Catal. Today* **2003**, *78*, 47-64.

(29) Desmedt, F.; Ganhy, J.-P.; Vlasselaer, Y.; Miquel, P. A catalyst for direct synthesis of hydrogen peroxide. WO Patent 2,013,068,340, **2013**.

(30) Carniti, P.; Gervasini, A. *Adsorp. Sci. Catal.* **2005**, *23*, 739-749.

(31) Carniti, P.; Gervasini, A. In *Calorimetry and Thermal Methods in Catalysis,* Auroux A., Ed.; Springer Series in Material Science, Springer, 2013; Vol. 154, p.p. 543-551.

(32) Zhu, H.; Zheng, Z.; Gao, X.; Huang, Y.; Yan, Z.; Zou, J.; Yin, H.; Zou, Q.; Kable, S.H.; Zhao, J.; Xi, J.; Martens, W.N.; Frost, R.L. *J. Am. Chem. Soc.* **2006**, *128*, 2373-2384.

(33) Ziolek, M. ; Sobczak I. *Catal. Today* **2017**, *285*, 211-225.

(34) Ziolek, M.; Decyk, P.; Sobczak, I.; Trejda, M.; Florek, J.; Golinska, H.; Klimas, W.; Wojtaszek, A. *Appl. Catal., A* **2011**, *391*, 194-204.

(35) Choudhary, T.V.; Banerjee, S.; Choudhary, V.R.; *Appl. Catal., A* **2002**, *234*, 1-23.

(36) Haneda, M.; Too, M.; Nakamura, Y.; Hattori, M. *Catal. Today* **2017**, *281*, 447-45.

(37) Melada, F.; Pinna, F.; Strukul, G.; Perathoner, S.; Centi, G. *J. Catal.* **2006**, *237*, 213-219.

(38) Wilson, N. M.; Flaherty, D. W. *J. Am. Chem. Soc.* **2016**, *138*, 574-586.

TABLES

Table 1. Summary of the Composition of Niobia-Silica Supports and Pd-Catalysts

sample code	preparation[a]	precursor	Nb (wt.%)	catalyst code	Pd (wt.%)
P-Nb$_4$S	co-precipitation	ANBO - TEOS	4.0	Pd$_{1.0}$/P-Nb$_4$S	1.0
P-Nb$_{6.2}$S	co-precipitation	NBE - TEOS	6.2	Pd$_{1.9}$/P-Nb$_{6.2}$S	1.9
P-Nb$_{6.5}$S	co-precipitation	ANBO - TEOS	6.5	Pd$_{1.2}$/P-Nb$_{6.5}$S	1.2
P-Nb$_{14.2}$S	co-precipitation	NBE - TEOS	14.2	Pd$_{1.4}$/P-Nb$_{14.2}$S	1.4
D-Nb$_{6.4}$S	deposition	NBE - silica[b]	6.4		
D-Nb$_{7.3}$S	deposition	NBE – silica[b]	7.3	Pd$_{1.6}$/D-Nb$_{7.3}$S	1.6
D-Nb$_9$S	deposition	NBE – silica[b]	9.05	Pd$_{1.4}$/D-Nb$_9$S	1.4

[a] For details: see paragraph *2.1.2. NbS Support Preparation, Experimental Section.*

[b] Silica supplied from Aldrich.

Table 2. Morphological Properties of Silica and Niobia-Silica Samples Determined from N_2 Adsorption-Desorption Isotherm Measurements

sample code	V_m [a] $(mL \cdot g^{-1})$	surface area $(m^2 \cdot g^{-1})$	pore volume [b] $(mL \cdot g^{-1})$	average pore size (nm)
Si	69.91	304	1.16	15.3
P-Nb$_4$S	100.1	436	0.24	2.21
P-Nb$_{6.2}$S	118.5	516	1.26	9.77
P-Nb$_{6.5}$S	16.33	71.1	0.28	15.6
P-Nb$_{14.2}$S	67.60	294	1.68	22.9
D-Nb$_{6.4}$S	71.22	311	0.99	12.8
D-Nb$_{7.3}$S	69.10	310	1.08	13.0
D-Nb$_9$S	64.09	279	1.02	14.5

[a] volume of N_2-gas adsorbed at monolayer, from BET linearized equation; [b] volume of liquid N_2 in the sample pores determined at P/P°=0.997.

Table 3. Acidic Properties of D-Nb$_{6.4}$S Surfaces Determined in Cyclohexane with PEA Molecular Probe by Pulse Experiment

sample code	surface area (m^2·g^{-1})	intrinsic acidity in cyclohexane (μequiv·g^{-1})	
		total sites	strong sites
D-Nb$_{6.4}$S	310	528	436 (83%)
D-Nb$_{6.4}$S/350/100	310	538	437 (81%)
D-Nb$_{6.4}$S/500/60	300	453	337 (74%)
D-Nb$_{6.4}$S/800/15	276	403	310 (77%)
D-Nb$_{6.4}$S/800/30	268	350	266 (76%)

SCHEMES and FIGURES

$$H_2O + \tfrac{1}{2}\,O_2 \quad \xleftarrow{\;k_2\;} \quad H_2 + O_2 \quad \xrightarrow{\;k_1\;} \quad H_2O_2$$

with H_2O_2 branching: $\xrightarrow{k_3} H_2O + \tfrac{1}{2}\,O_2$ and $\xrightarrow[k_4]{H_2} 2\,H_2O$
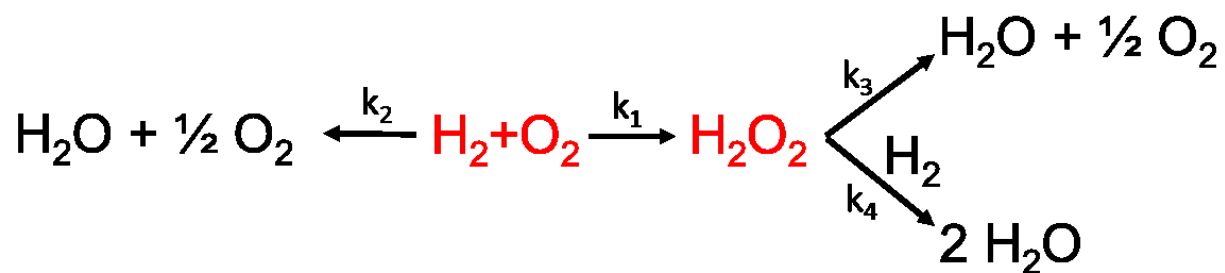
Scheme 1. Main reactions involved in the process of direct synthesis of H_2O_2 (DS) from gaseous H_2 and O_2 mixture: two parallel reactions (k_1 and k_2 rate constants) from H_2 and O_2 reagents and two consecutive reactions (k_3 and k_4 rate constants) from the main product (H_2O_2) formed are shown.
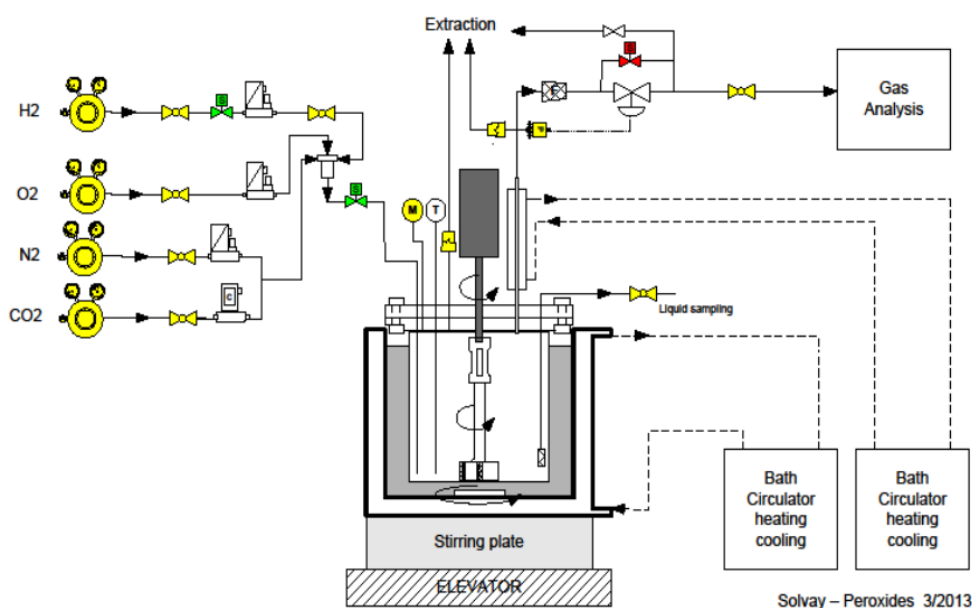
Figure 1. Reaction line used for the tests of DS synthesis of H_2O_2 in liquid-phase: it comprises the semi-batch slurry catalytic reactor into which the formed products could accumulate in the liquid phase while the fed gas mixture (H_2, O_2, and N_2) continuously flowed out from the reactor. Typical conditions used: H_2 concentration; 3.60%, O_2 concentration; 55%, pressure, $5 \cdot 10^3$ kPa (in methanol) or 10^4 kPa (in water); temperature, 5°C; solvent, methanol (150 ml) or water (100 ml).
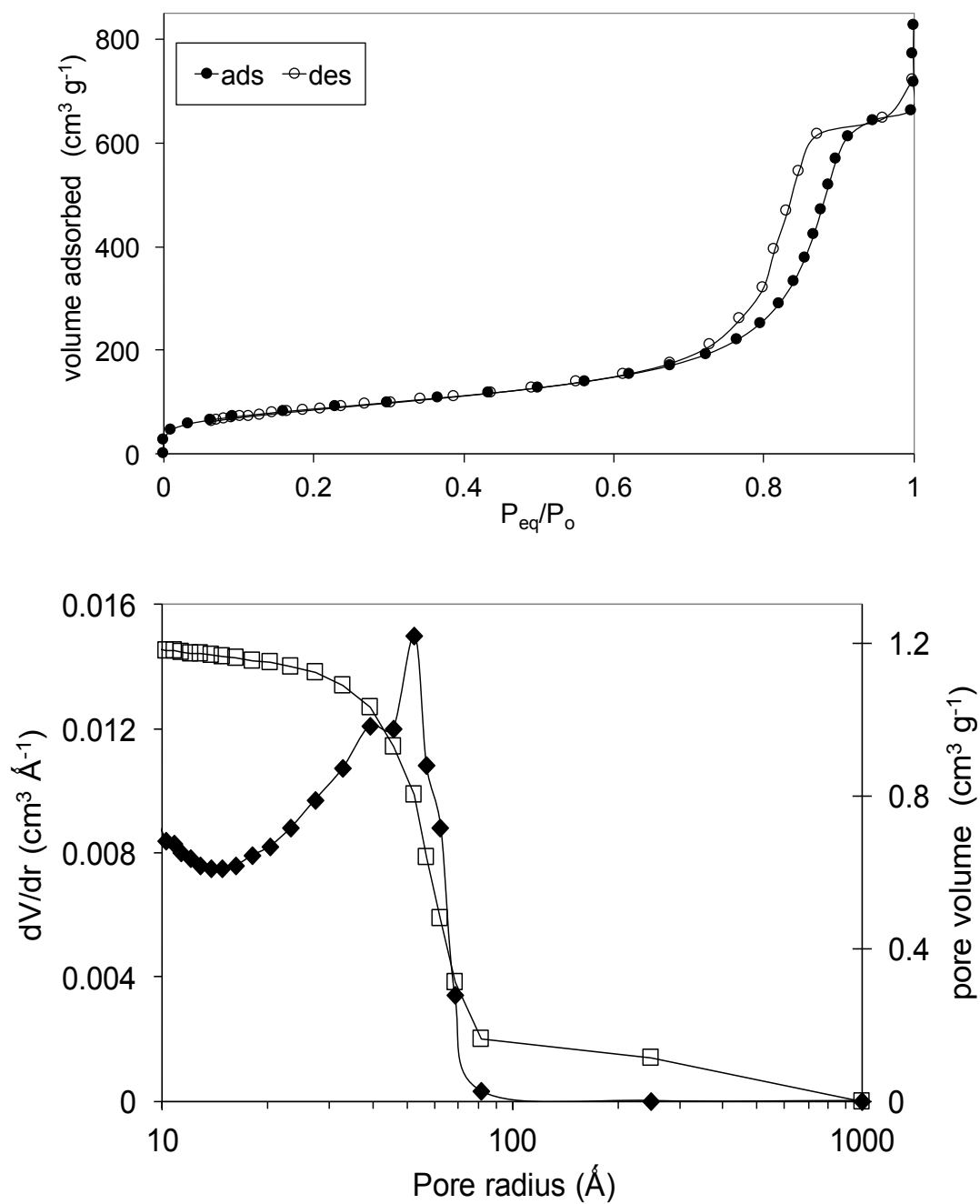
Figure 2. N$_2$ adsorption (full marks) and desorption (empty marks) isotherms on D-Nb$_{6.4}$S (top) and pore size distribution (dV/dr) and pore volume as a function of pore radius, computed according with BJH model on the N$_2$ desorption branch (bottom).
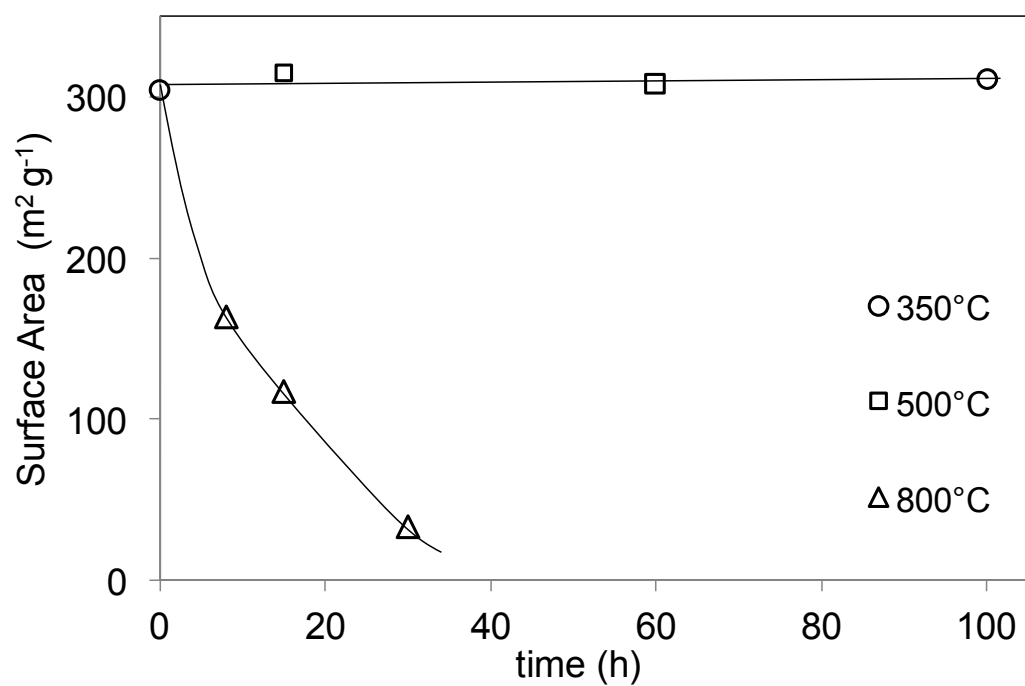
Figure 3. Trends of surface area of silica (S) sample after thermal treatments of ageing at three different temperatures for different times.
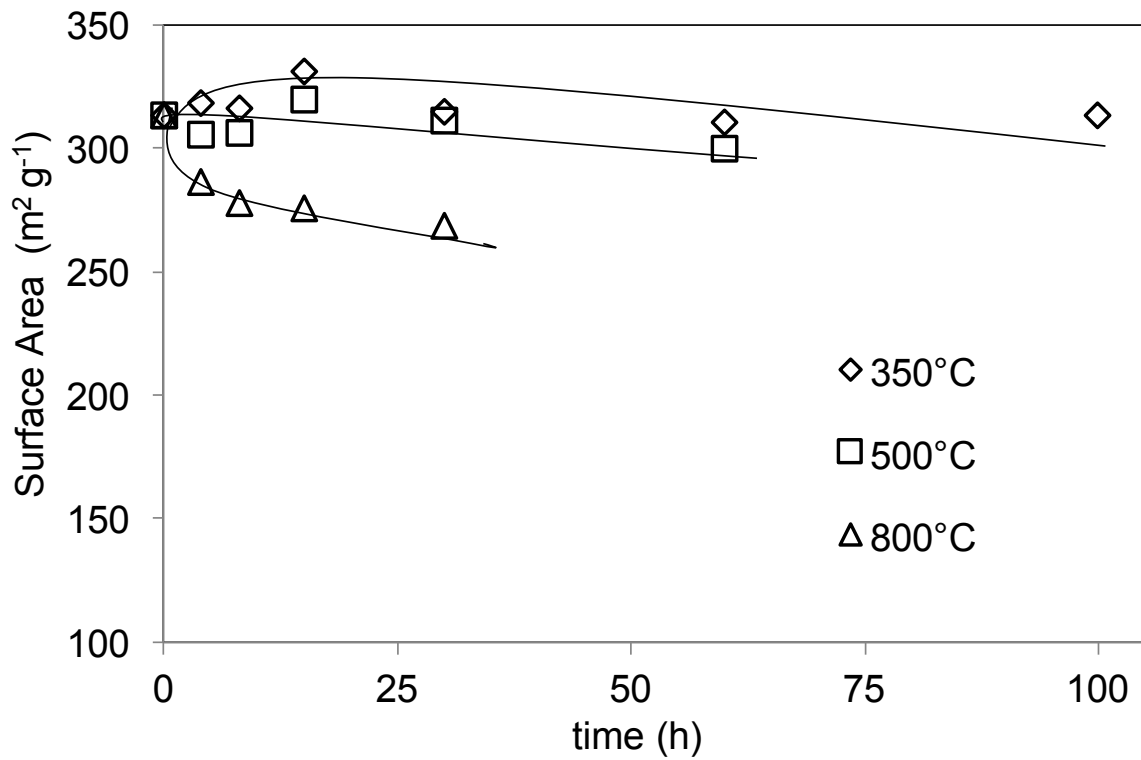
Figure 4. Trends of surface area values of D-Nb$_{6.4}$S (prepared from NBE deposited on silica) after thermal treatments of ageing at three different temperatures for different times.
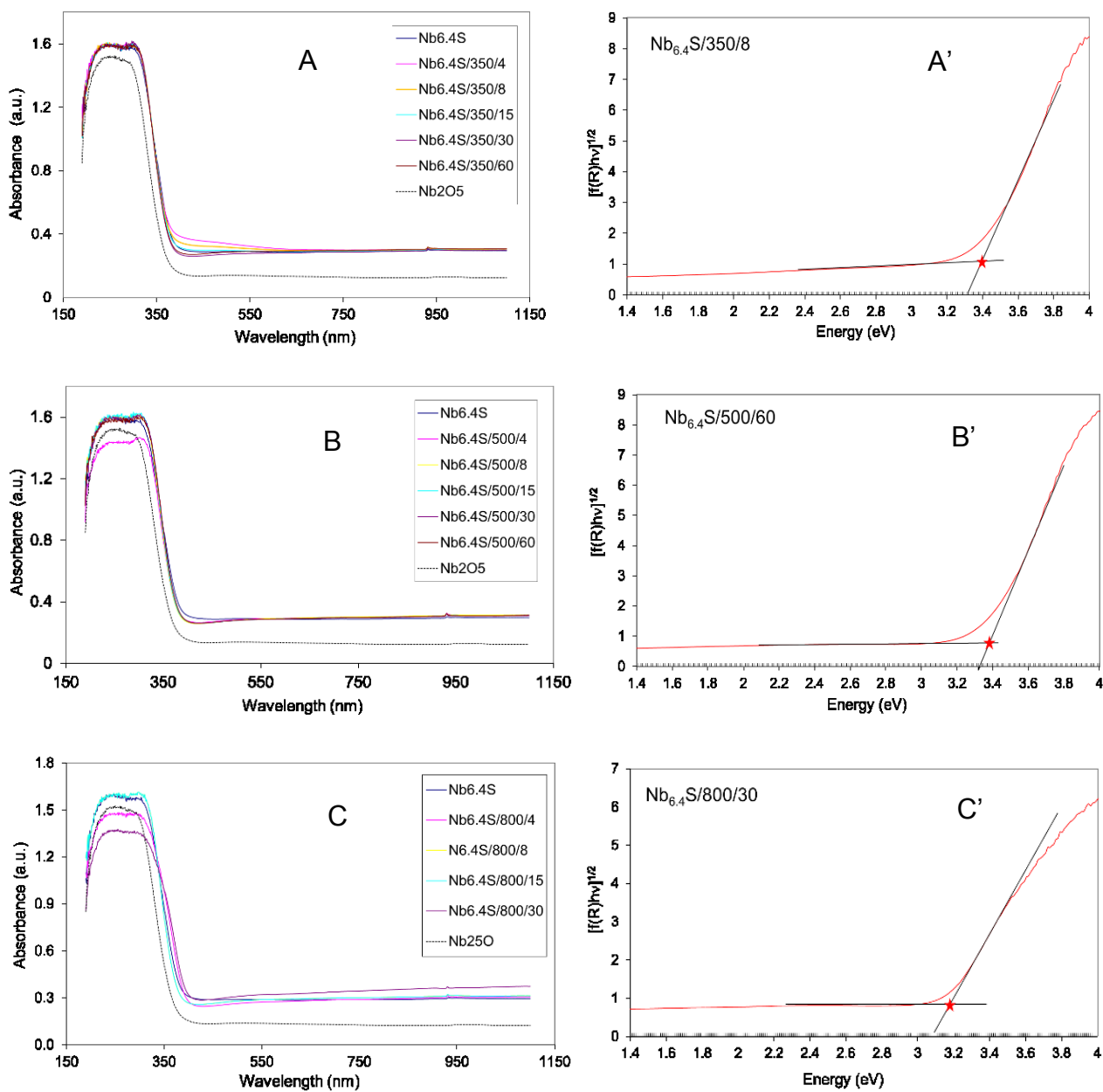
Figure 5. UV-vis DRS spectra of D-Nb$_{6.4}$S sample aged at 350°C (A), 500°C (B), and 800°C (C) for different times (left) and Tauc plots of one representative chosen sample for each temperature: 350°C (A'); 500°C (B'), and 800°C (C') (right). Nb$_2$O$_5$ (from CBMM, Brazil) has been used as reference material.
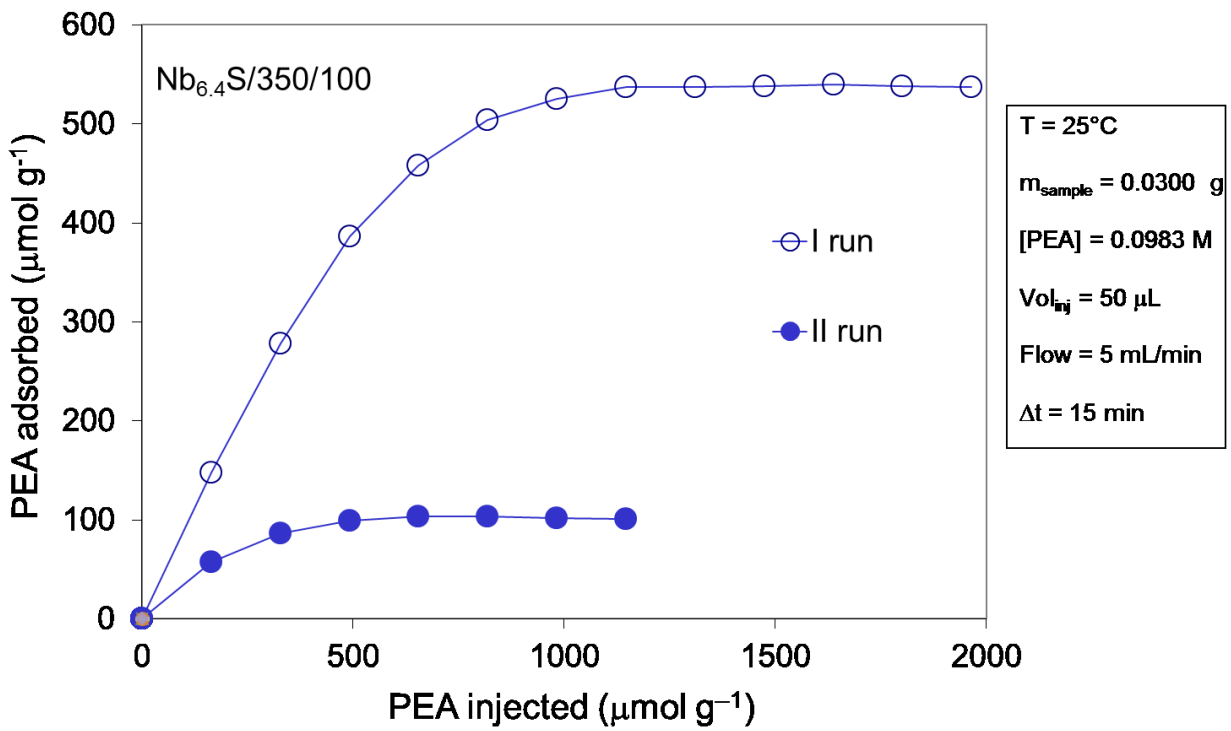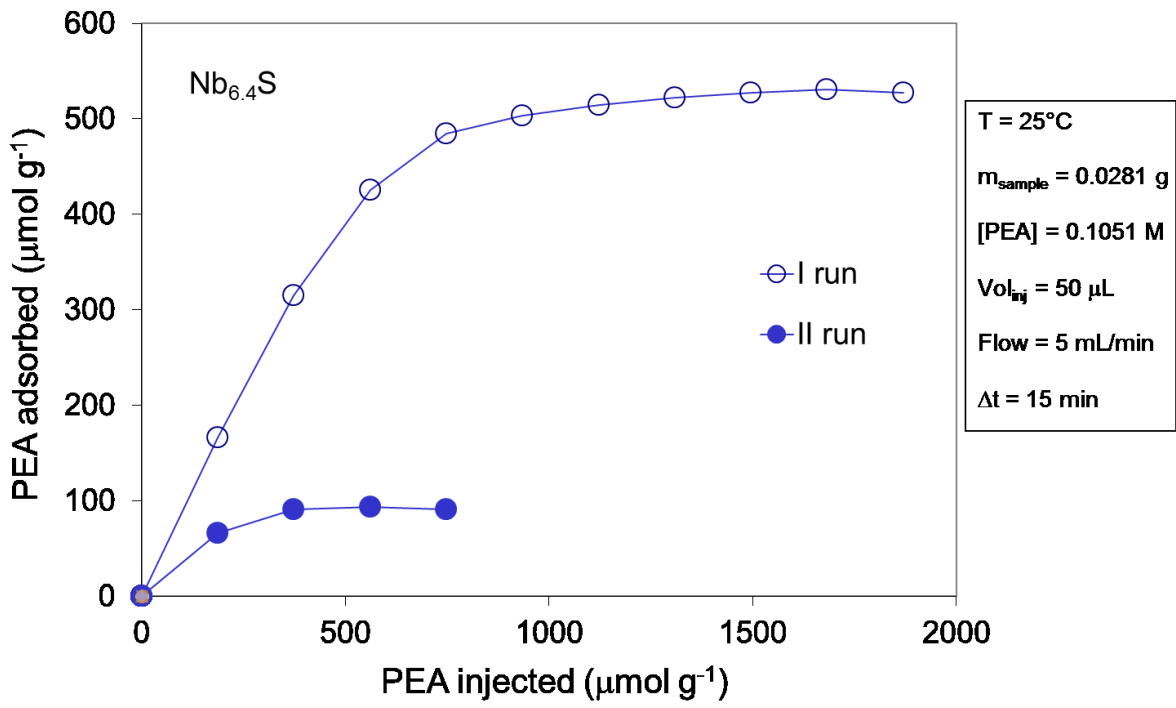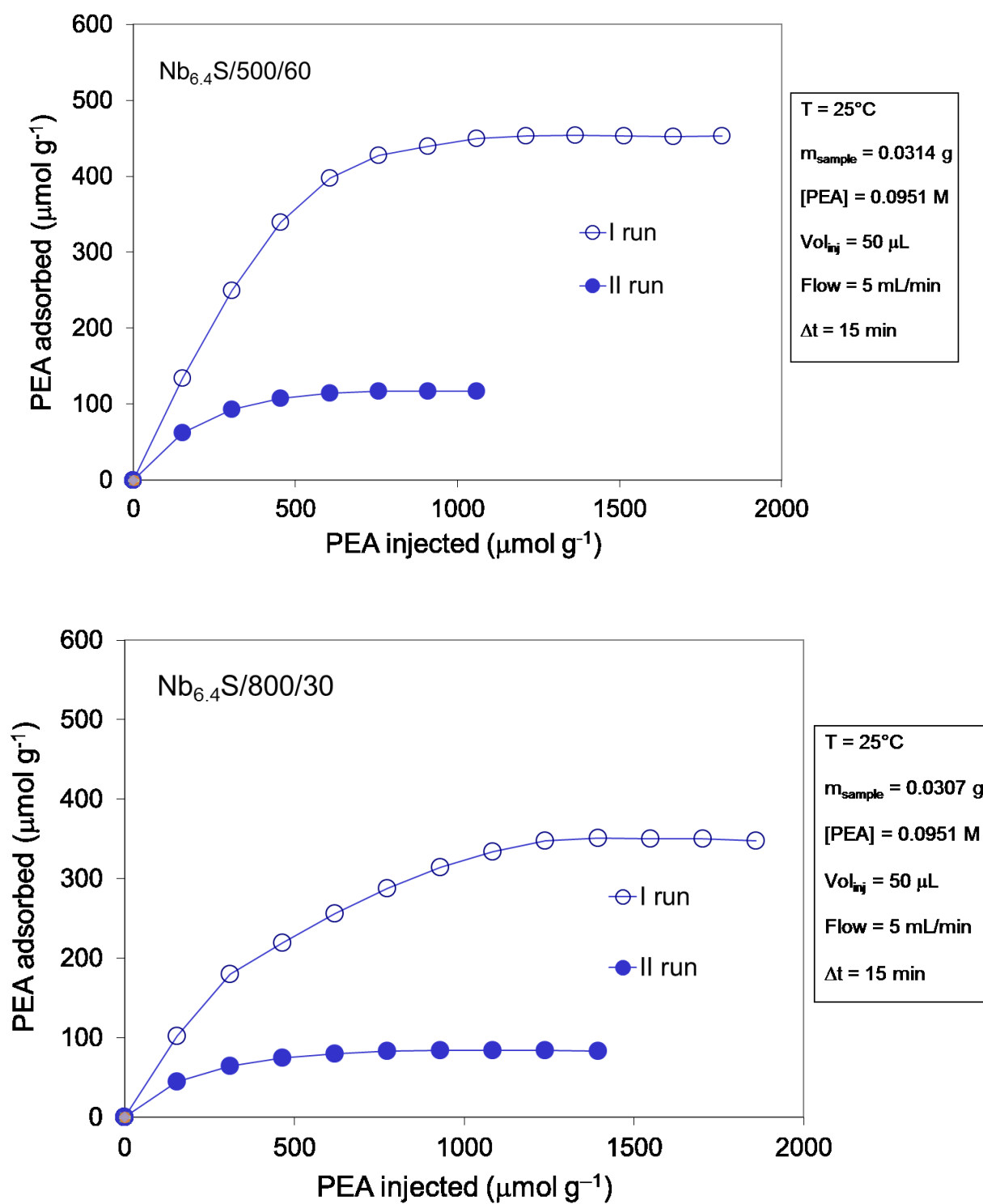
Figure 6. Determinations of *intrinsic* acidity of D-Nb$_{6.4}$S, D-Nb$_{6.4}$S/350/100, D-Nb$_{6.4}$S/500/60, and D-Nb$_{6.4}$S/800/30, measured in cyclohexane by PEA adsorption with pulse-method experiments (I°, open markers, and II°, full markers, runs are shown).
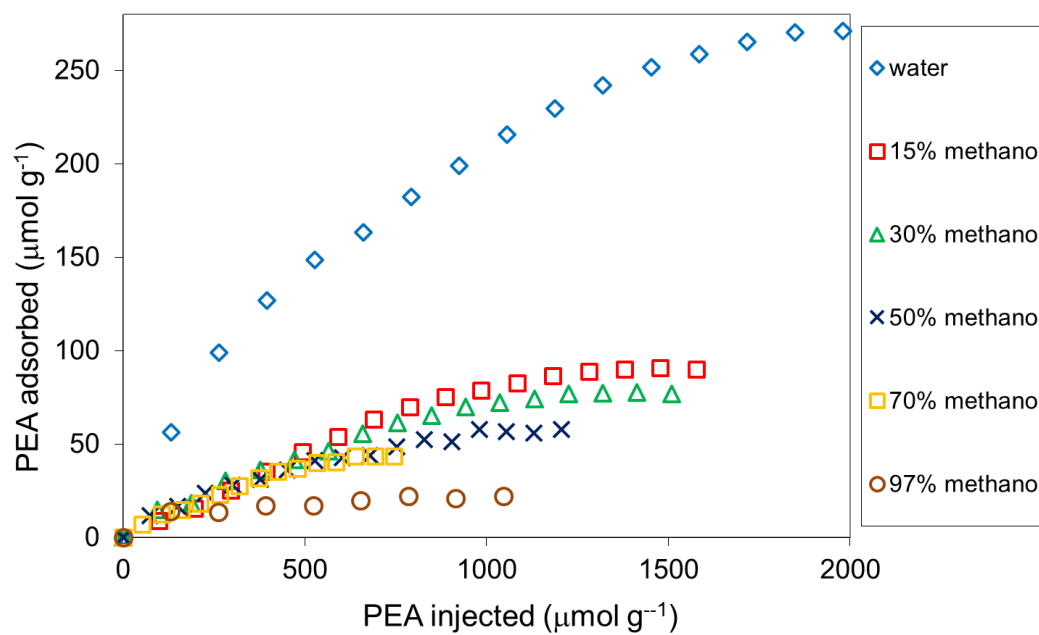
Figure 7. *Effective* acidity determinations of D-Nb$_{6.4}$S measured in water and water-methanol solutions by PEA adsorption with pulse-method experiments (only I° run is shown).
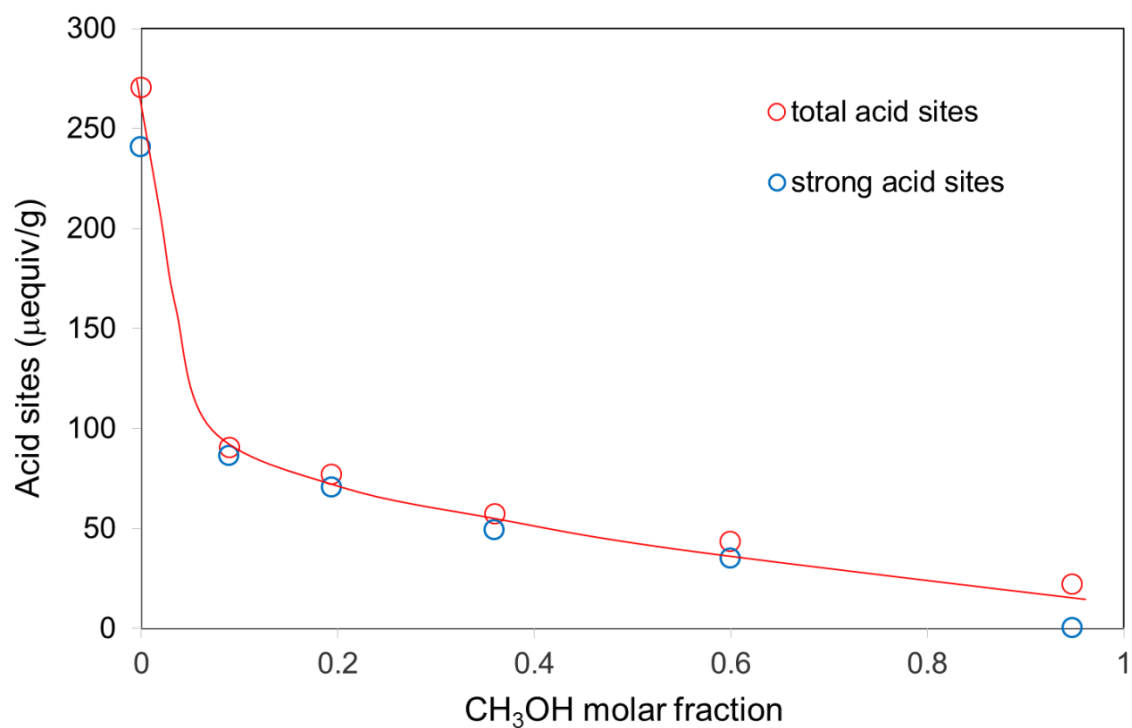
Figure 8. Evolution of the e*ffective* acidity of D-Nb$_{6.4}$S as a function of methanol molar fraction; measurements performed by PEA adsorption with pulse-method experiments.
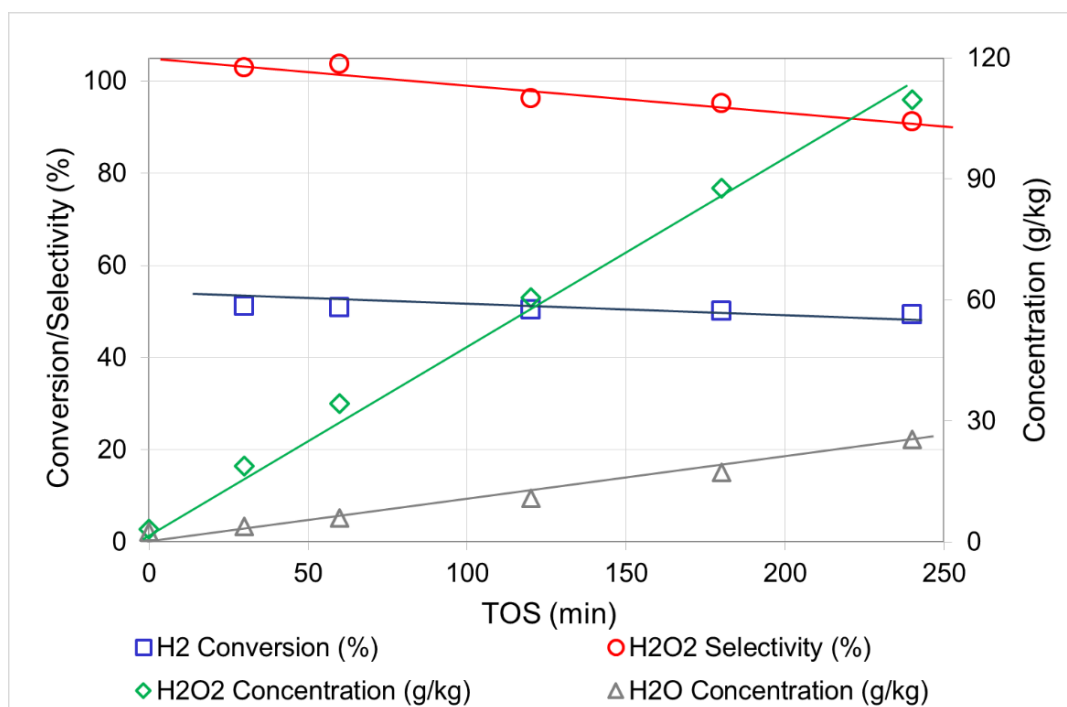
Figure 9. Typical results observed in the catalytic synthesis of H_2O_2 from H_2 and O_2 gas mixture as a function of time on stream; typical conditions: reaction temperature, 5°C; total pressure, $5 \cdot 10^3$ kPa (in methanol) or 10^4 kPa (in water).
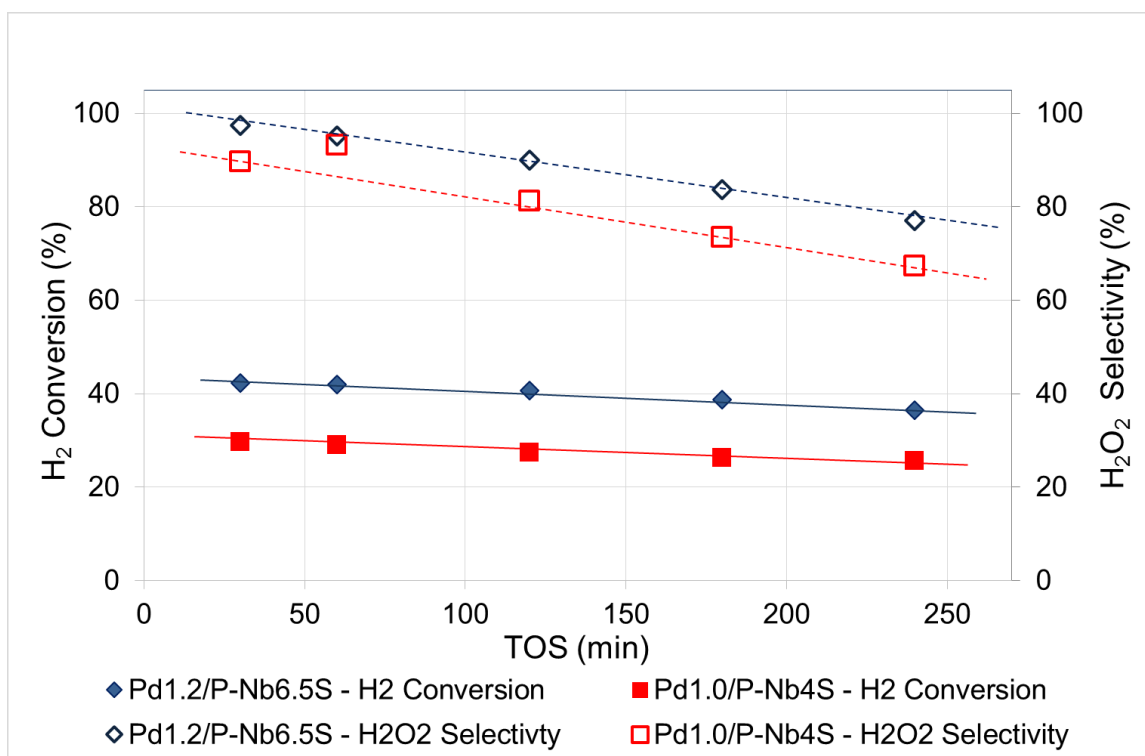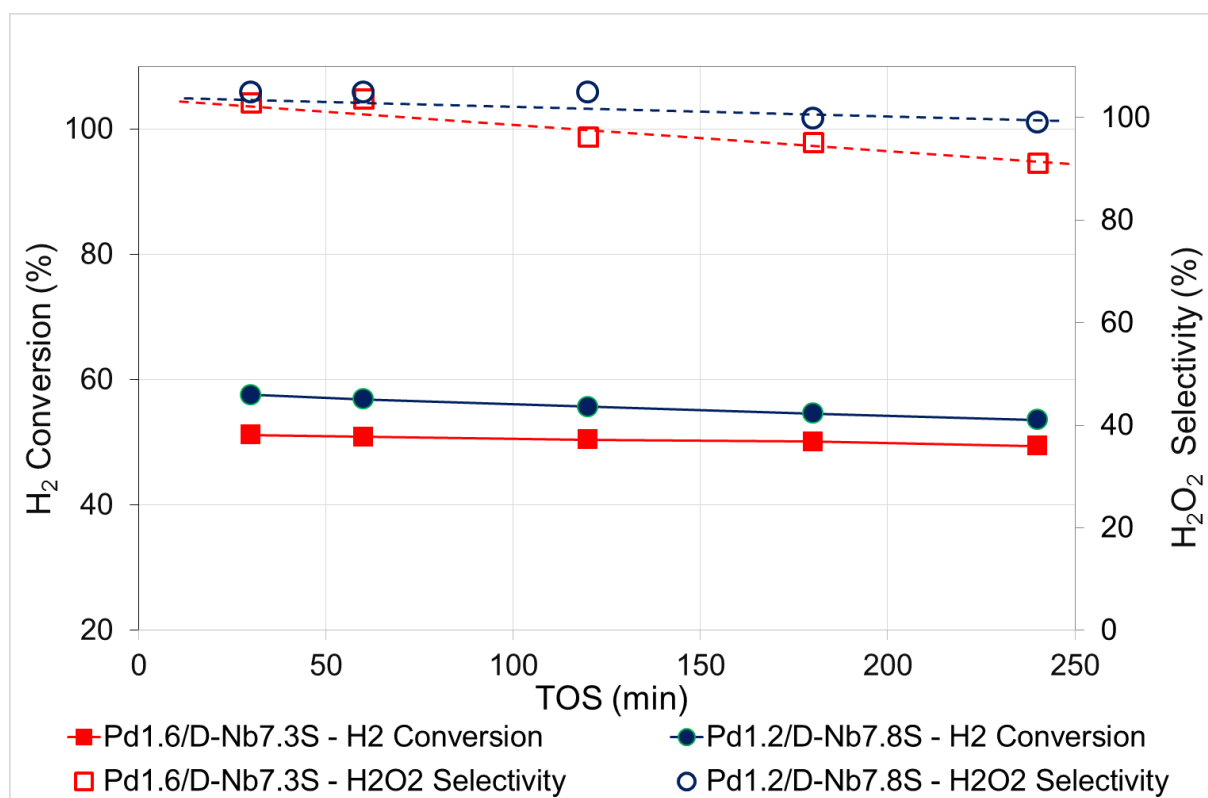
Figure 10. Catalytic synthesis of H_2O_2 in methanol (150 ml) from H_2 and O_2 mixture as a function of time on stream on $Pd_{1.2}/P-Nb_{6.5}S$ and $Pd_{1.0}/P-Nb_4S$ catalysts; typical conditions: reaction temperature, 5°C; pressure, $5 \cdot 10^3$ kPa.

Figure 11. Catalytic synthesis of H_2O_2 in methanol (150 ml) from H_2 and O_2 mixture as a function of time on stream on $Pd_{1.6}$/D-Nb$_{7.3}$S and $Pd_{1.4}$/D-Nb$_9$S catalysts; typical conditions: reaction temperature, 5°C; pressure, 5 10^3 kPa.
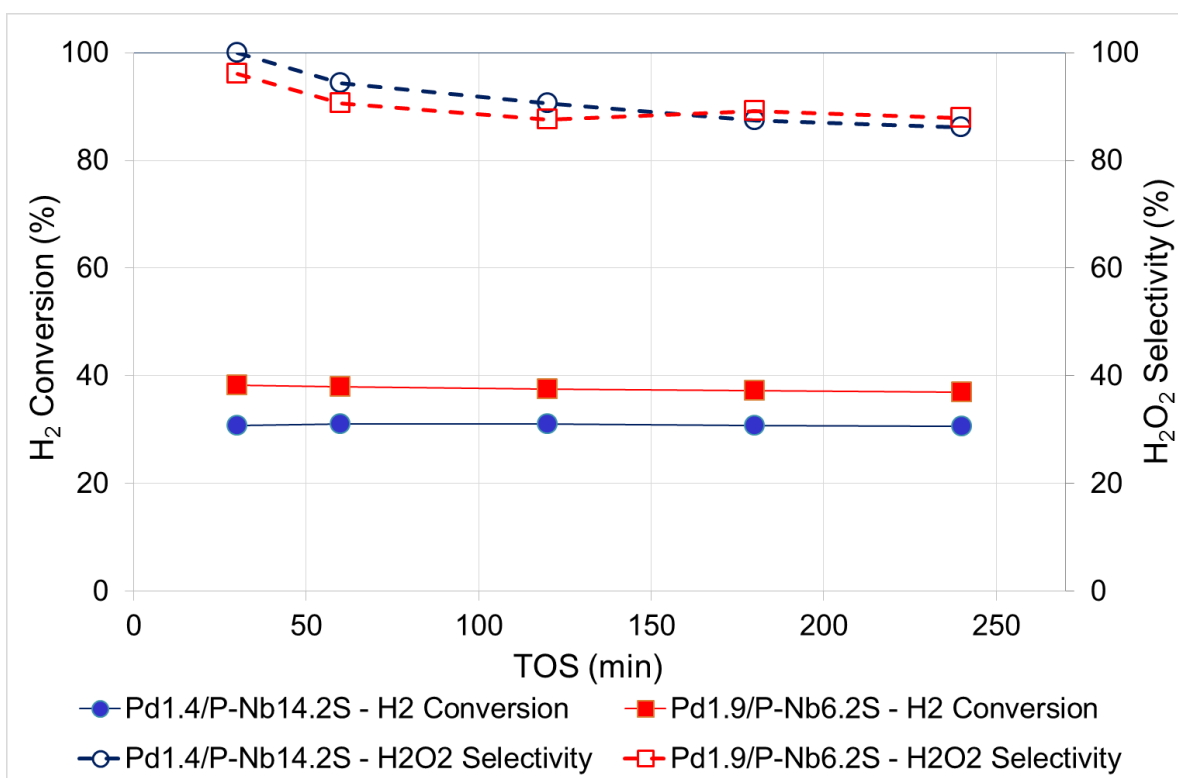
Figure 12. Catalytic synthesis of H_2O_2 in water (100 ml) from H_2 and O_2 mixture as a function of time on stream on $Pd_{1.4}/P\text{-}Nb_{14.2}S$ and $Pd_{1.9}/P\text{-}Nb_{6.2}S$ catalysts; typical conditions: reaction temperature, 5°C; solvent, pressure, 10^4 kPa.

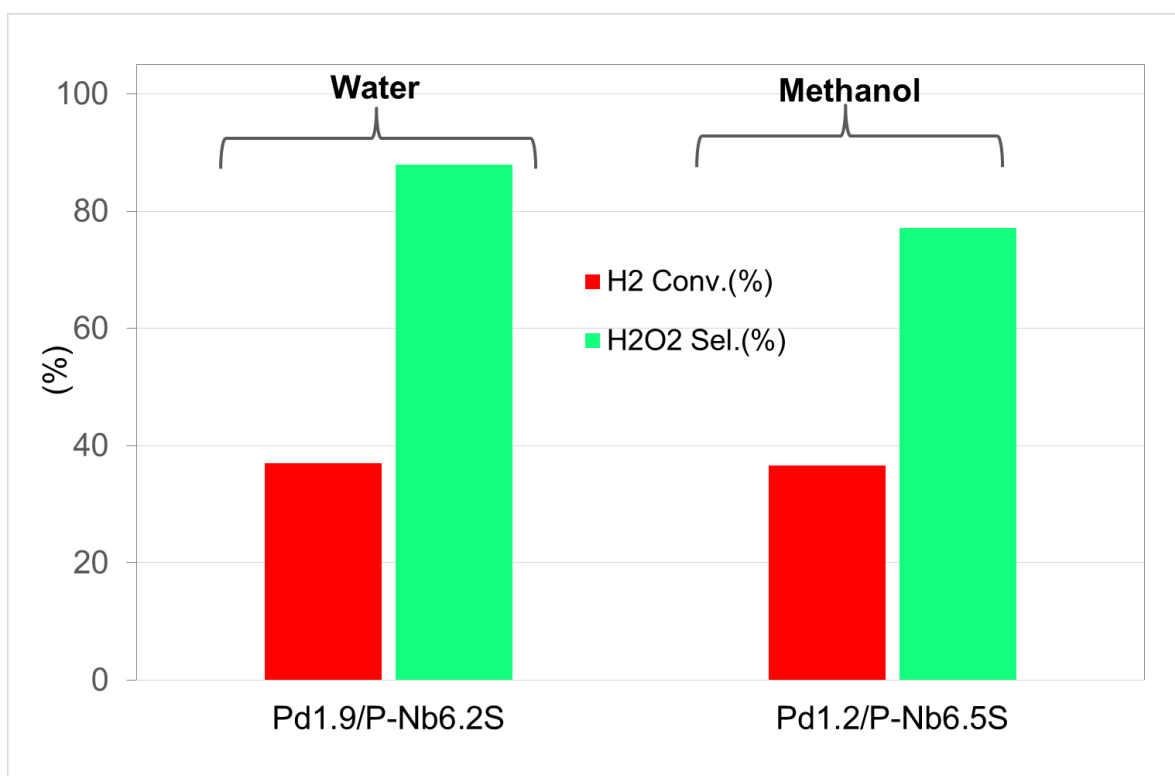**Figure 13.** Comparison of H_2 conversion and H_2O_2 selectivity in the H_2O_2 DS between $Pd_{1.9}/P$-$Nb_{6.2}S$ (in water, 100 ml and 10^4 kPa) and $Pd_{1.2}/P$-$Nb_{6.5}S$ (in methanol, 150 ml and $5\ 10^3$ kPa) after 4 h of reaction; reaction temperature 5°C.
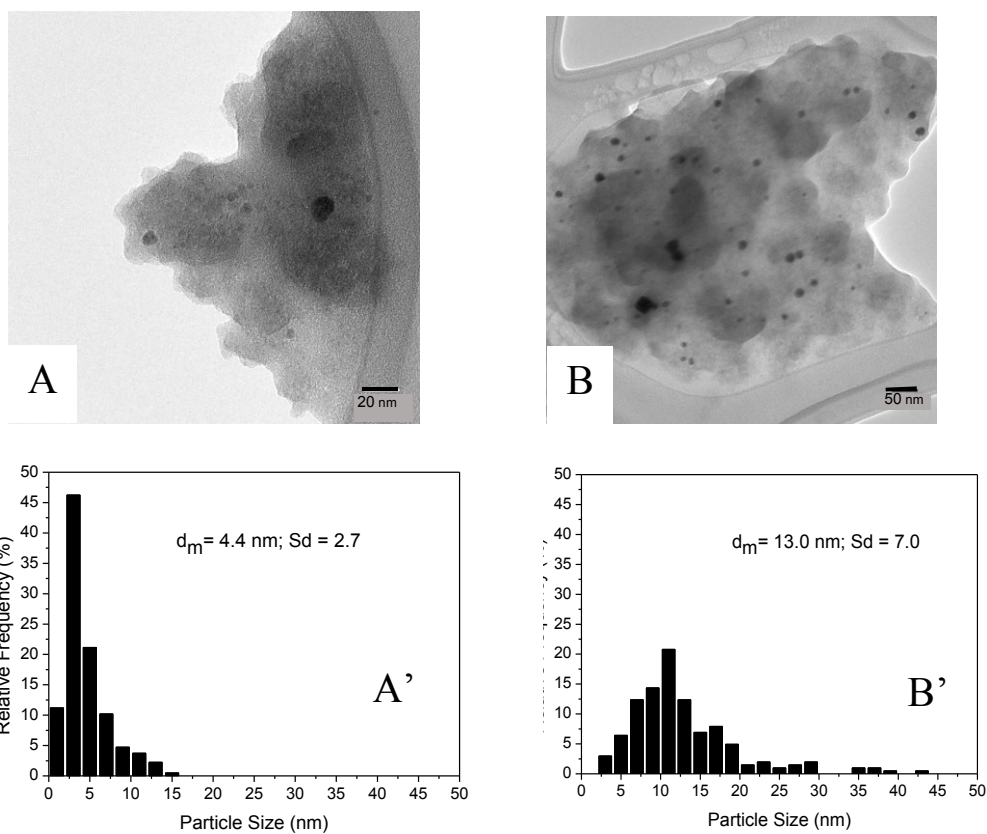
Figure 14. TEM images of Pd$_{1.6}$/D-Nb$_{7.3}$S, fresh (A) and used (B) surfaces with relevant statistical distributions (A' and B') of the Pd-particles calculated from the observation of more than 500 nanoparticles.